

Comments and associated responses for:

Processes influencing heat transfer in the near-surface ice of Greenland's ablation zone

Benjamin H. Hills et al. 2018

Minor Revisions

Author responses are in blue.

Hills et al. 2018: Processes influencing heat transfer in the near-surface ice of Greenland's ablation zone

The main concerns of both reviewers addressed the definition of the metric T_0 , consistent depth referencing of observed and calculated vertical profiles, aspects of forcing data and lower boundary condition and enhanced discussion of subsurface refreezing processes. Overall, the manuscript was substantially improved with respect to these issues, thanks for that effort. The following comments address some remaining issues which I suggest to reconsider in more detail.

Thank you for this review. We agree that the manuscript was substantially improved from the previous revisions, and hope that the changes addressed below satisfy your final concerns. As you state above, the primary concerns of consistent depth referencing and subsurface refreezing were a focus of the previous revisions. The remaining concerns seem to focus on the boundary conditions at the surface and the bottom of our model domain. We hope that the response below gives some validation in our choice for boundary conditions.

1) Line above P2L15: I am still not confident regarding " T_0 ", which is the essential metric used in this work. Here the authors state "Seasonal air temperature oscillations are diminished with depth into the ice, until they are negligible (i.e. $\sim 1\%$) at a 'depth of zero annual amplitude'. On the other hand it is stated that "The mean value from the lowermost sensor (analogous to T_0) is -3.2 at 27-km , ... (P4L19, which refers to actual evaluation practice)". Methodically seen this leaves kind of gap i.e., to show that at this lowermost sensor position the 1% criterium is actually matched (on average at least). Additionally this issue also questions in what extent the pragmatic choice of the lowermost sensor position is justified in view of the fact that right this level is intrinsically influenced by the lower boundary condition (where no temperature variability can occur by definition). Hence this question indirectly leads back to the one whether the simulations should not build on a deeper domain. I still recommend performing a sensitivity study addressing these issues and related uncertainties.

We assess the $\sim 1\%$ criterion in a section added to the supplement.

The lower boundary is a Neumann boundary condition, rather than a Dirichlet boundary condition as suggested in the comment above ("where no temperature variability can occur by definition"). The temperature at the bottom of the domain can therefore change in time, but we run the model "with a one-day time step until ice temperature at the bottom of the domain converges to a steady temperature" (as stated on P8L8).

In order to address concerns with the lower boundary, we have run additional tests presented in a section added to the supplement.

2) I recognize the added details concerning the meteorological data. Concerning the ice temperature measurements close to the surface some critical remarks may be given, though. If thermistors were housed in a “black casing” (as stated now, P3L30), than not only sensors lying at the surface may have been affected by solar induced heating. Dark cables/casing can experience significantly enhanced temperature and effect sensors (also by conduction within cables due to temperature gradients). Glendinning and Morris (1999) demonstrated for snow that corresponding effects can be of order $>2^{\circ}\text{C}$ @70cm depth. The indicated "discarding" procedure helps identifying problems close to 0°C , but does not identify/correct effects on sensors having negative temperatures. Overall one might expect that thermistors in the upper ca. 50cm below the surface are prone to a warm bias during summer (which can not be excluded by observations that at a certain point of time cables were found frozen into the ice.

We do not agree that the discarding procedure is only satisfactory for measurements close to 0°C . All values, no matter the temperature measured, are discarded after the sensor lies on the surface (as stated at P3L30).

We argue that the results presented here and the story given in the discussion are illustrated by the entire temperature profile measured to 20 m and are mostly independent of any small errors within the uppermost ~ 0.5 m. Having said that, we have modified the statement to convey a loss of confidence in the measurements as they approach the surface:

“Because each temperature sensor is in a black casing, measurement error surely increases due to solar heating as sensors move into the rotten cryoconite layer (~ 0.2 m depth), and we completely discard any measurement taken after the sensor is exposed at the surface.”

3) The authors multiply mention that the paper is not focussing on meteorological aspects, which is fine. However, this not acceptable regarding observed air temperature which constitutes essential model input and is used in context of interpretation of the results. I recognize more detailed information on used instruments and their setup. But the potential influence of a likely inefficient radiation shield on the temperature measurements is still understated. According to the now given Fig. S2, a rather ineffective shield was used and significant radiation errors may be expected (also because being mounted close i.e., ca. 0.5m to the strongly reflecting surface and the low incidence angle of solar radiation during transitional seasons). There are several studies incl. manufacturer statements, that this kind of screen can induce significant errors in temperature measurements (several $^{\circ}\text{C}$ depending on wind speed, too). Unfortunately, these effects are hard to quantify or to correct. At least, however, one expects some more critical comments that such uncertainties are inherent in the data and were not corrected. The currently used air temperature data are likely to be too high, which shall be discussed in the interpretation of the results, too.

Comparison to PROMICE data is ok (Fig. S4) is not really valuable in this context (due large distance between sites and respective need to correct for elevation differences). Regarding calculation of surface temperatures, the used emissivity shall be specified.

We appreciate these concerns with the air temperature measurement. We do agree that there are potential problems, especially in that the sensor location remains fixed as the surface melts instead of maintaining at 2-m distance. The most appropriate way to address this is through a comparison to what is considered a more sophisticated AWS station.

We added a statement in the manuscript pointing out this comparison:

“Out of concern for error in our air temperature measurement, we offer a comparison (Figure S4) to the nearby weather station monitored by the Programme for Monitoring of the Greenland Ice Sheet (PROMICE) (van As et al., 2012).”

Figure S4 was added to address a concern from the original review. We argue that while it is not a perfect comparison, it gives some justification in using our measured air temperature as a surface boundary condition.

Added to supplement:

“and considering ice a black body radiator.”

4) Revision of Fig. 2 is acknowledged, however, I still can not fully agree to the argument that different i.e. inconsistent record lengths do not affect calculation of T_0 (“... should be comparable because it is below any seasonal variation ..”)

We address the robustness of T_0 in the section added to the supplement.

Further the caption mentions " For field sites at which the air temperature was measured for at least a full year, a dashed line shows the mean air temperature". Why then still showing dashed lines for b, de and f, which do not cover a full year?

The statement is true as it stands in the manuscript. The *air temperature* was measured at those sites for over one year. For these strings that you mention, the *ice temperature* was not measured for more than one year, but that has already been addressed at several places in the manuscript including in this figure caption.

Overall, I do not fully support diverse arguments why uncertainties in air temperature measurements and its use as model input is not an issue in context of this investigation. But I also see the weak point that the available data hardly allow a better approach. In this perspective, corresponding sensitivity studies could have been valuable. This is meant in sense of disturbing input (i.e., air temperature) and investigate the impact on simulation results (T_0 basically).

As we stated in the original review, this study is focused on processes within the ice. We argue that the requested sensitivity studies for the surface boundary condition would detract from the overall story presented here. As stated above, we tried to ease some of these concerns about the surface boundary condition by comparing our measurements to the nearby KAN_L weather station. A thorough investigation of the atmospheric processes effecting this surface boundary condition is best left for a separate study. We acknowledge that our meteorological instruments, while appropriate for this study of heat transfer in ice, are not state-of-the-art and therefore leave room for error in the atmospheric interpretation. We have added statements in the manuscript addressing the concerns with our instrumentation (see comments above), and suggest that if an

intensive study of the atmospheric processes is to be done it should be done by a group that focuses primarily on meteorological data.

5) P5L16: "...Net radiation is less than zero in the winter (net outgoing because of thermal emission in the infrared wavelengths)", may be reformulated to account for the fact that not only emission counts, but that this component emission prevails over atmospheric input)

Changed to:

"(net outgoing because thermal emission in the infrared wavelengths dominates over atmospheric inputs)"

6) P6L8: "... model uses measured meteorological variables as the surface boundary condition and simulates ice temperature to 21 m, a depth chosen for consistency with measured data. The ice temperature at the depth of zero annual amplitude, T0, is output from the bottom of the domain for each model experiment and used as a metric..." Admittently, I am still not convinced about several aspects in this context as long as respective uncertainties are not addressed quantitatively. In particular this concerns use of air temperature as forcing at the upper boundary (ignoring measurements uncertainties and stratification effects) and the implementation of the lower boundary condition at a depth close to the depth of average T0. Both is still rather superficial treated.

We have addressed these issues in our revision and throughout this response. Our approach to air temperature is not fundamentally different than many other studies in Greenland. We utilize modern and high quality instrumentation for measurement, and the paper acknowledges potential shortcomings of the data and methods. We provide a comparison to the nearby KAN_L station, which does not reveal an intrinsic flaw with our data.

We show in the section added to the supplement that our modeling procedure of the lower boundary condition does in fact, have no impact on our results (see below).

P9L4: I need some help how of Phi(rad) in given dimensions is compatible with equ.1

Changed to $\phi_{rad} = \frac{Q}{0.2m}$ (instead of cm) for clarity. The units are

$$\begin{aligned} [Q] &= W/m^2 \\ [\phi_{rad}] &= W/m^3 \\ \left[\frac{\phi_{rad}}{\rho_i} \right] &= \frac{J}{kg\ s} \end{aligned}$$

Which is the time rate of change of the specific enthalpy (as a source term).

P10L15: "The limiting cases show that this bottom boundary condition strongly controls the near-surface temperature, with a range in the resulting T0 values from -17.0°C to -2.0°C. In summary, measured ice temperatures are consistently warmer than both the measured air temperature and simulated ice temperature ..." This is an expected and most important result, which has to be re-emphasized in the discussions, too. And again, it would be most interesting to know in what extent this issue depends on alternative depth of the model domain and corresponding specification of the lower boundary condition.

We feel that this result has been given appropriate emphasis in the discussion. The subsurface gradient is the focus of section 5.1.

We address problems with the lower boundary condition in the section added to the supplement. Unfortunately, we cannot include these limiting gradients in the deeper tests, because the gradients are specifically prescribed based on measured values at ~20 m depth. Setting a Neumann boundary with the specified gradient at 50 m instead would give a different result, not because the model is wrong but because that is a completely different scenario.

Processes influencing heat transfer in the near-surface ice of Greenland's ablation zone

Benjamin H. Hills^{1,2}, Joel T. Harper², Toby W. Meierbachtol², Jesse V. Johnson³, Neil F. Humphrey⁴, Patrick J. Wright^{5,2}

¹Department of Earth and Space Sciences, University of Washington, Seattle, Washington, USA

²Department of Geosciences, University of Montana, Missoula, Montana, USA

³Department of Computer Science, University of Montana, Missoula, Montana, USA

⁴Department of Geology and Geophysics, University of Wyoming, Laramie, Wyoming, USA

⁵Inversion Labs LLC, Wilson, Wyoming, USA

Correspondence to: Benjamin H. Hills (bhills@uw.edu)

Abstract. To assess the influence of various heat transfer processes on the thermal structure of ice near the surface of Greenland's ablation zone, we compare *in-situ* measurements with thermal modeling experiments. A total of seven temperature strings were installed at three different field sites, each with between 17 and 32 sensors and extending up to 21 meters below the surface. In one string, temperatures were measured every 30 minutes, and the record is continuous for more than three years. We use these measured ice temperatures to constrain our modeling experiments, focusing on four isolated processes and assessing the relative importance of each for the near-surface ice temperature: 1) the moving boundary of an ablating surface, 2) thermal insulation by snow, 3) radiative energy input, and 4) subsurface ice temperature gradients below the seasonally active near-surface layer. In addition to these four processes, transient heating events were observed in two of the temperature strings. Despite no observations of meltwater pathways to the subsurface, these heating events are likely the refreezing of liquid water below 5-10 meters of cold ice. Together with subsurface refreezing, the five heat transfer mechanisms presented here account for measured differences of up to 3°C between the mean annual air temperature and the ice temperature at the depth where annual temperature variability is dissipated. Thus, in Greenland's ablation zone, the mean annual air temperature is not a reliable predictor of the near-surface ice temperature, as is commonly assumed.

Deleted: mechanisms

Deleted: emperature

Deleted: highly resolved

Deleted:

Deleted: simplified

Deleted: S

Deleted: separate

Deleted: analyses

Deleted: ed

1 Introduction

Bare ice regions of the Greenland ice sheet have high summer melt rates. Here, the surface ice temperature is important to ablation processes such as melt, water storage, runoff, and albedo modifications associated with the surface cryoconite layer. The ice surface temperature also acts as an essential boundary condition for the transfer of heat into deeper ice below, and is therefore important for ice flow modeling (e.g. Meierbachtol et al., 2015) as well as interpretation of borehole temperature measurements (Harrington et al., 2015; Hills et al., 2017; Lüthi et al., 2015). In order to constrain the rate of ice melting, and more generally to understand the mechanisms which move energy between the ice and the atmosphere above, we must understand the processes that control near-surface heat transfer in bare ice.

Heat transfer at the ice surface is dominated by thermal diffusion from the overlying air (Cuffey and Paterson, 2010). Seasonal air temperature oscillations are diminished with depth into the ice, until they are negligible (i.e. $\sim 1\%$) at a 'depth of zero annual amplitude' (van Everdingen, 1998). The exact location of this depth is dependent on the thermal diffusivity of the material through which heat is conducted as well as the period of oscillations (Carslaw and Jaeger, 1959; pp. 64-70). In theory, the temperature at the depth of zero annual amplitude, a value we will call T_0 , is approximately constant and equal to the mean annual air temperature. In snow and ice, the depth of zero annual amplitude is approximately 10 and 15 m respectively (Hooke, 1976). For this reason, studies in the cryosphere often use T_0 as a proxy for the mean air temperature, drilling to 10 or more meters to measure the snow or ice temperature at that depth (Loewe, 1970; Mock and Weeks, 1966).

In places where heat transfer is purely diffusive, the snow or ice is homogeneous, and interannual climate variations are minimal, T_0 is a good approximation for the mean air temperature. However, prior studies have shown that, in many areas of glaciers and ice sheets, the relationship between air and ice temperatures can be substantially altered by additional heat transfer processes. For example, in the percolation zone, infiltration and refreezing of surface meltwater warm the subsurface (Humphrey et al., 2012; Müller, 1976). Studies have also revealed ice anomalously warmed by 5°C or more in the ablation zone (Hooke et al., 1983; Meierbachtol et al., 2015), but the mechanisms for this are unclear.

Hooke et al. (1983) explored the impacts of several heat transfer processes within near-surface ice at Storglaciären and the Barnes Ice Cap. They focused on the wintertime snowpack which acts as insulation to cold air temperatures but is permeable to meltwater percolation. Their results showed that the average ice temperature at and below the equilibrium line of those glaciers tends to be higher than the mean annual air temperature. They attributed the observed difference mainly to snow insulation because the strength of their measured offset was correlated to the thickness of the snowpack.

In this study, we expand the analysis of Hooke et al. (1983) and turn focus to the GrIS ablation zone with near-surface temperature profiles from seven locations. We use our temperature measurements in conjunction with a one-dimensional model to assess heat transfer processes in this area. The processes which make the ablation zone different from other areas of a glacier or ice sheet are, first, that the ice surface spends much of the summer period pinned at the melting point, despite slightly warmer air temperatures. Next, high ablation rates counter emergent ice flow, removing the ice surface and exposing deeper ice, along with its heat content, to the surface. The contrast of a

Deleted: heat transfer

Deleted: ing

wintertime snowpack to bare ice in the summer enables an insulating effect during winter months. The deep penetration of solar radiation into bare ice results in subsurface heating and melting (Brandt and Warren, 1993; Liston et al., 1999). Finally, surface melt can move through open fractures, carrying latent heat with it to deeper and colder ice, and upon refreezing, the meltwater warms that ice below the surface (Jarvis and Clarke, 1974; Phillips et al., 2010).

Our near-surface temperature observations represent an aggregated sum of the processes mentioned above. A numerical model can be used to partition the relative importance of those processes, but only with measurements in hand as validation. Therefore, confidently constraining the role of near-surface heat transfer processes requires temperature measurements with both high temporal and spatial resolution, and records that span hours to seasons.

2 Field Site and Instrumentation

Field observations used in this study are from three sites in western Greenland (Fig. 1). Each site is named by its location with respect to the terminus of Isunnguata Sermia, a land-terminating outlet glacier. The equilibrium line altitude is at about 1500 m elevation in this area (van de Wal et al., 2012), which is 400 m above the furthest inland site, 46-km, so all sites are well within the ablation zone and ablation rates are high (2-3 m/yr). Solar radiation in the summer creates a layer of interconnected cryoconite holes at the ice surface, and water moving through that cryoconite layer converges into surface streams. There are no large supraglacial lakes in the immediate area of any site; all streams eventually drain from the surface through moulines. A series of dark folded layers emerge to the ice surface in this region of the ice sheet (Wientjes and Oerlemans, 2010).

At each field site, boreholes for temperature instrumentation were drilled from the surface to between 10 and 21 m depth using hot-water methods. In total, seven strings of temperature sensors were installed – one at both sites 27-km and 46-km in 2011, followed by five at site 33-km between 2014 and 2016. Strings are named by the year they were installed. Each consists of between 17 and 32 sensors spaced at 0.5-3.0 m along the cable (Table 1). In 2011 and 2014, thermistors were used as temperature sensors. The thermistors have measurement resolution of 0.02°C and accuracy of about 0.5°C after accounting for drift (Humphrey et al., 2012). In subsequent years, we used a digital temperature sensor (model DS18B20 from Maxim Integrated Products, Inc.). This sensor has resolution 0.0625°C and about the same accuracy as the thermistors. To increase accuracy, each sensor was lab-calibrated in a 0°C bath, and field-calibrated with a temperature measurement during freeze-in (borehole water is exactly 0°C).

Because each temperature sensor is in a black casing, measurement error surely increases due to solar heating as sensors move into the rotten cryoconite layer (~0.2 m depth), and we completely discard any measurement taken after the sensor is exposed at the surface.

Meteorological variables were measured at each field site as well. In this study, we use the near-surface (~2-m) air temperature (Vaisala HMP60 with a radiation shield), the net radiative heat flux over all wavelengths shorter than 100 μm (Kipp and Zonen NR Lite), and the change in surface elevation measured with a sonic distance sensor (Campbell SR50A). Data from the sonic distance sensor are filtered manually, removing any obvious outliers (more than 0.5 m from the surrounding measurements). The filtered data are then partitioned into two variables,

Deleted: the

Deleted: ure

Deleted: s are

Deleted: ed

Deleted: when

Deleted: lies on the surface

Deleted: to the sun

cumulative ablation during the melt season and changes in snow depth during the winter. An automated weather station with all the above instrumentation was mounted on a fixed pole frozen in the ice, with segments being removed from the mounting pole each summer so the instrumentation remains close to the surface and does not extend significantly into the air temperature inversion (Miller et al., 2013). [Out of concern for error in our air temperature measurement, we offer a comparison \(Fig. S4\) to the nearby weather station monitored by the Programme for Monitoring of the Greenland Ice Sheet \(PROMICE\) \(van As et al., 2012\).](#) The measurement frequency for meteorological data varies from ten minutes to an hour, but all data are collapsed to a daily mean for input to a heat transfer model.

In addition to ice temperature and meteorological measurements, investigations of the subsurface were completed at site 33-km with a borehole video camera and a high-frequency ground-penetrating radar survey ([see Supplement](#)). These investigations were carried out in pursuit of what we think may have been subsurface fractures that are not expressed at the ice surface (described in section 5.2). With five temperature sensor strings, an automated weather station, and the subsurface investigations, site 33-km is by far the most thoroughly studied of the three sites. For that reason, measurements from this site serve as the foundation for the model case study presented in section 4.

3 Results

3.1 Observed Ice Temperature

Near-surface ice temperatures were measured through time in seven shallow boreholes at three different field sites ([Fig. 2](#)). [Although hot-water drilling methods temporarily warm ice near the instrumentation, the ice around these shallow boreholes cools to its original temperature within days to weeks.](#) Measured temperatures are spatially variable between sites. The mean value from the lowermost sensor (analogous to T_0) is -3.2 at 27-km, -8.6 at 46-km, and from -9.7°C to -8.1 at 33-km. In all cases, measured T_0 values are warmer than the mean annual air temperature. Temperature gradients are calculated by fitting a line to the mean temperature of the four lowermost sensors for each string. These gradients are also variable, typically being between -0.15 and 0.0°C/m but +0.16°C/m at the 27-km field site (positive being increasing temperature with depth below the surface). As expected, the direction of temperature gradients measured here correlate with those measured in the uppermost ~100 m for full-thickness temperature profiles (Harrington et al., 2015; Hills et al., 2017).

Even the five temperature profiles measured at site 33-km exhibit some amount of spatial variability. Three temperature strings, T-15a, b, and c, are all similar, having strong negative temperature gradients (approximately -0.14°C/m), and cold T_0 temperatures (-9.6°C). [Close to the surface, these three temperature strings are cold](#) compared to the others. However, those strings stopped collecting measurements in May 2017 and did not yield a full year of data. The missing summer period explains the strong positive temperature gradient near the surface for those three strings. T-16 is the shortest string, extending to only 9.5 m depth. This short string exhibits the smallest range in temperatures throughout a season with the coldest surface temperatures not even reaching -15°C. In terms of mean temperature, T-16 is similar to T-14, having a small negative temperature gradient and warm temperatures in comparison to those of T-15 [a, b, and c](#). Based on our observations, spatial variability in near-surface ice

Deleted: see s

Deleted: station

Deleted: ure

Deleted: approximately

temperature at site 33-km is controlled on the scale of hundreds of meters. Proximal observations from the nearby T-15a, b, and c strings are similar to one another, but greater variability is observed when including the more distant strings, T-14 and T-16.

Closer inspection of the measured temperature record through time reveals the transient nature of near-surface ice temperature (Fig. 3). As expected, these data show a strong seasonal oscillation near the surface. During the melt season, the ice surface quickly drops as ice is warmed to the melting point. Just below the surface, the winter cold wave persists for several weeks into the summer season. In string T-14 we observe delayed freeze-in behavior in one sensor (Fig. 3b) and transient heating events during the melt seasons (Fig. 3c, 3d, 3e). Similar heating events were observed in string T-16 (Fig. 4), but not in any other. The events range in magnitude, but in one instance ice is warmed from -10°C to -2°C in 2 hours (Fig. 3c). We can only speculate on the origins of these events, and address this below in section 5.2.

3.2 Meteorological Data

Meteorological data from site 33-km were observed over three years (Supplement Fig. S4). Air temperatures are normally at or above the melting temperature during the summer but fall to below -30°C in winter months. The measured ablation rate is 2-3 m/yr and maximum snow accumulation is only up to 0.5 m. Net radiation is less than zero in the winter (net outgoing because thermal emission in the infrared wavelengths dominates over atmospheric inputs) but over 100 W/m² (daily mean) on some days in the summer.

The mean air temperature over the entire measurement period at site 33-km (-10.5°C) is cold in comparison to measured ice temperatures at that site (Fig. 2; T-14, T-15a, T-15b, T-15c, and T-16). This warm anomaly between the ice and air temperature is also observed at sites 27-km and 46-km, where ice is warmer than the measured air temperature and significantly warmer than the reference from a regional climate model (Meierbachtol et al., 2015). Interestingly, we measure almost no winter snowpack at sites 27-km and 46-km due to low precipitation and strong winds during the time period over which those data were collected (2011-2013). Our observations are thus in contradiction to the inferences made by Hooke et al. (1983) in Arctic Canada, where the offset between air and ice temperature appeared to be primarily a result of snow insulation.

Overall, the three years for which meteorological data were collected are significantly different. The 2014-15 winter was particularly cold, bringing the mean air temperature of that year more than a degree lower than the other two seasons. Snow accumulation was approximately doubled that winter in comparison to the other two. Also, the summer melt season is longer in 2016 than in 2015. In comparison with past trends from the nearby PROMICE station, KAN L, the second year is more typical for this area (van As et al., 2012). To model a representative season, data from that second year (July 2015 to July 2016) were chosen as annual input for the model case study.

4 Analysis

Our objective is now to investigate how various processes active in Greenland's ablation zone influence T_b . In order for model results to achieve fidelity, inputs and parameters need to be representative of actual conditions. We therefore use the meteorological data to constrain the modeling experiments. Our modeling is focused at field site

Deleted: three

Deleted: ure

Deleted: For this particular

Deleted: s

Deleted: ,

Deleted: ,

Deleted: was observed

Deleted: ure

Deleted: were observed

Deleted: ure

Deleted: the T-16

Deleted: ure

Deleted: ure

Deleted: s

Deleted: ary

Deleted: ure

Deleted: of

Deleted: ure

Deleted: a

Deleted: site

33-km, where we have the most data for constraining the problem.

4.1 Model Formulation

The foundation for quantifying impacts of near-surface heat transfer processes is a one-dimensional thermodynamic model. We argue that the processes tested here are close enough to being homogeneous that they can be adequately assessed in one dimension. The one exception is the measured heating events which are transient and spatially discrete, these are discussed in section 5.2 and are not included in the model analysis. Our model uses measured meteorological variables as the surface boundary condition and simulates ice temperature to 21 m, a depth chosen for consistency with measured data. The ice temperature at the depth of zero annual amplitude, T_0 , is output from the bottom of the domain for each model experiment and used as a metric to compare net temperature changes between simulations. The model, its boundary conditions, and the experiments are all designed to test heat transfer processes within the ice itself. To maintain focus on ice processes, we ignore any atmospheric effects above the ice surface such as turbulent heat fluxes. The model does not, nor is it meant to, simulate the surface mass balance.

We implement an Eulerian framework, treating the z dimension as depth from a moving surface boundary so that emerging ice is moving through the domain and is removed when it melts at $z = 0$. We use a finite element model with a first-order linear element and 0.5-m mesh spacing refined to 2 cm near the surface. For a seamless representation of energy across the water/ice phase boundary, we implement an advection-diffusion enthalpy formulation (i.e. Aschwanden et al., 2012; Brinkerhoff and Johnson, 2013),

$$(\partial_t + w\partial_z)H = \partial_z(\alpha\partial_z H) + \phi/\rho_i \quad (1)$$

Here, ∂ is a partial derivative, t is time, w is the vertical ice velocity with respect to the lowering ice surface, z is depth, H is specific enthalpy, α is thermal diffusivity, ϕ is any added energy source, and ρ_i is the density of ice. The diffusivity term is enthalpy-dependent,

$$\alpha(H) = \begin{cases} k_i/\rho_i C_p & \text{cold, } H < H_m \\ v/\rho_i & \text{temperate, } H > H_m \end{cases} \quad (2)$$

where k_i is the thermal conductivity of ice which we assume is constant over the small temperature range in this study ($\sim 25^\circ\text{C}$), C_p is the specific heat capacity which is again assumed constant, v is the moisture diffusivity in temperate ice, and H_m is the reference enthalpy at the melting point (all constants are shown in Table 2).

Aschwanden et al. (2012) include a thermally diffusive component in temperate ice (i.e. $k_i\partial_z^2 T_m(P)$). However, since we consider only near-surface ice, where pressures (P) are low, this term reduces to zero. Using this formulation, energy moves by a sensible heat flux in cold ice and a latent heat flux in temperate ice. We assume that the latent heat flux, prescribed by temperate ice diffusivity (v/ρ_i in equation (2)), is an order of magnitude smaller than the cold ice diffusivity ($k_i/\rho_i C_p$). We argue that this is representative of the near-surface ice when cold ice is impermeable to meltwater.

The desired model output is ice temperature. It has been argued that temperature is related to enthalpy through a continuous function, where the transition between cold and temperate ice is smooth over some 'cold-temperate

Deleted: -

Deleted: a

transition surface' (Lüthi et al., 2002). On the other hand, we argue that cold ice is impermeable to water except in open fractures (which we do not include in these simulations), so we use a stepwise transition,

$$T(H) = \begin{cases} (H - H_m)/C_p + T_m & \text{cold} \\ T_m & \text{temperate} \end{cases} \quad (3)$$

Additional enthalpy above the reference increases the water content in ice,

$$\omega(H) = \begin{cases} 0 & \text{cold} \\ (H - H_m)/L_f & \text{temperate} \end{cases} \quad (4)$$

where L_f is the latent heat of fusion. If enough energy is added to ice that its temperature would exceed the melting point, excess energy goes to melting. In our case study, we limit the water content based on field observations of water accumulation in the layer of rotten ice and cryoconite holes. This rotten cryoconite layer extends to approximately 20-cm depth and as an upper limit accumulates a maximum 50% liquid water. Therefore, we limit the water content in the rotten cryoconite layer,

$$0.0 \leq \omega \leq 0.5 \quad (5)$$

with any excess ~~melting~~ immediately leaving the model domain as surface runoff.

The two boundary conditions are 1) fixed to the air temperature at the surface,

$$T(\text{surface}, t) = T_{air} \quad (6)$$

and 2) free at the bottom of the domain,

$$\frac{\partial T}{\partial z_{bottom}} = 0.0 \quad (7)$$

Both boundary conditions are with no liquid water content, $\omega = 0$. The surface boundary condition is updated at each time step to match the measured air temperature. The bottom boundary condition is fixed in time. This bottom boundary condition is also changed for some model experiments to test the influence of a temperature gradient at the bottom of the domain (section 4.2.4).

4.2 Experiments

Four separate model experiments are run, each with a new process incorporated into the physics, and each guided by observational data. All simulations use the enthalpy formulation above rather than temperature in order to track the internal energy of the ice/water mixtures that are prevalent in the ablation zone. ~~The results from each experiment~~ are referenced to an initial control run, ~~which is~~ simple thermal diffusion of the measured air temperature in the absence of any additional heat transfer processes. Meteorological data are input where needed for an associated process in the model. These data are clipped to one full year and input at the surface boundary in an annual cycle. The model is run with a one-day time step until ice temperature at the bottom of the domain converges to a steady

Deleted: water

Deleted: E

Deleted: is

Deleted: which reflects

temperature. A description of each of the model experiments follows below. These experiments build on one another, so each new experiment incorporates the physics of all previously discussed processes.

4.2.1 Ablation

The first experiment simulates motion of the ablating surface. While the control run is performed with no advective transport (i.e. $w = 0$), in this experiment we incorporate advection by setting the vertical velocity equal to measurements of the changing surface elevation through time. When ice melts the ice surface location drops. Because the vertical coordinate, z , in the model domain is treated as a distance from the moving surface, ablation brings simulated ice closer to the surface boundary. Hence, the simulated ice velocity, w , is assigned to the ablation rate (except in the opposite direction, ice moves upward) for this first model experiment. The ablation rate is calculated as a forward difference of the measured surface lowering.

4.2.2 Snow Insulation

The second experiment incorporates measured snow accumulation, which thermally insulates the ice from the air. The upper boundary condition is now assigned to the snow surface, whose location changes in time. Diffusion through the snowpack is then simulated as an extension of the ice domain but with different physical properties. The thermal conductivity of snow (Calonne et al., 2011),

$$k_s = 2.5 * 10^{-6} \rho_s^2 - 1.23 * 10^{-4} \rho_s + 0.024 \quad (8)$$

is dependent on snow density, ρ_s , for which we use a constant value, 300 kg/m^3 . We treat the specific heat capacity of snow to be the same as ice (Yen, 1981).

4.2.3 Radiative Energy

The third model experiment incorporates an energy source from the net radiation measured at the surface. Energy from radiation is absorbed in the ice and is transferred to thermal energy and to ice melting (van den Broeke et al., 2008). We assume that all this radiative energy is absorbed in the uppermost 20 cm, the rotten cryoconite layer, and if snow is present the melt production immediately drains to that cryoconite layer. When the net radiation is negative (wintertime) we assume that it is controlling the air temperature, so it is already accommodated in our simulation; thus, the radiative energy input is ignored in the negative case. This radiative source term is incorporated into

equation (1) at each time step, $\phi_{rad} = \frac{Q}{0.2m}$, where Q is the measured radiative flux at the surface in W/m^2 . All constants for the rotten cryoconite layer are the same as that for ice.

While some models treat the absorption of radiation in snow/ice more explicitly with a spectrally-dependent Beer-Lambert Law (Brandt and Warren, 1993), we argue that it is reasonable to assume all wavelengths are absorbed near the surface over the length scales that we consider. The only documented value that we know of for an absorption coefficient in the cryoconite layer is 28 m^{-1} (Llibouty, 1965) which is close to that of snow (Perovich, 2007). If the properties are truly similar to that of snow, about 90 percent of the energy is absorbed in the uppermost 20 cm

Deleted: 0c

Deleted: that

(Warren, 1982). Moreover, we argue that this is precisely the reason that the cryoconite layer only extends to a limited depth; it is a result of where radiative energy causes melting.

4.2.4 Subsurface Temperature Gradient

Finally, in the fourth model experiment we change the boundary condition at the bottom of the domain. The free boundary is changed to a Neumann boundary with a gradient of $-0.05^{\circ}\text{C}/\text{m}$, a value that approximately matches the measured gradient at site 33-km. Importantly, this simulated gradient is in the same direction, although with a larger magnitude, of the upper ~ 100 m of ice in our measurements of deep temperature profiles (Hills et al., 2017). In this case, the advective energy flux is upward, but the temperature gradient is negative, bringing colder ice to the surface. In addition, two limiting cases were tested, with gradients of $\pm 0.15^{\circ}\text{C}/\text{m}$. This is the approximate range in measured gradients (Fig. 2).

Deleted: ure

4.3 Model Results

The control model run of simple thermal diffusion predicts that ice temperature converges to approximately the mean annual air temperature of the study year (-9.9°C) by about 15 m below the ice surface. This result is in agreement with the analytical solution (Carslaw and Jaeger, 1959), but slightly different from the mean air temperature (-9.6°C) because the air can exceed the melting temperature in the summer while the ice cannot. Other atmospheric effects such as turbulent heat fluxes and the thermal inversion could also cause a difference between measured air temperature and ice surface temperature, but these are not considered here. For each model treatment, 1-4, the incorporation of an additional physical process changes the ice temperature. Differences between model runs are compared using T_0 at 21 m. Again, the model experiments are progressive, so each new experiment includes the processes from all previous experiments. Key results from each experiment are as follows (Fig. 5):

Deleted: damps

1. Diffusion alone results in $T_0 = -9.9^{\circ}\text{C}$, whereas observed temperatures range from -9.7°C to -8.1 at the 33-km field site.
2. Because the ablation rate is strongest in the summer, the effect of incorporating ablation is to counteract the diffusion of warm summer air temperatures. The result is a net cooling of T_0 from experiment (1) by -0.92°C .
3. Snow on the ice surface insulates the ice from the air temperature. In the winter, snow insulation keeps the ice warmer than the cold air, but with warm air temperatures in the spring it has the opposite effect. Because snow quickly melts in the springtime, the net effect of snow insulation is substantially more warming than cooling. T_0 for this experiment is $+0.78^{\circ}\text{C}$ warmer than the previous.
4. Radiative energy input mainly controls melting (van den Broeke et al., 2008), but incorporating this process does warm T_0 by $+0.52^{\circ}\text{C}$.
5. Imposing a $-0.05^{\circ}\text{C}/\text{m}$ temperature gradient at the bottom of the model domain, consistent with observation, dramatically changes T_0 by -2.5°C .

Deleted: ure

Both ablation and the subsurface temperature gradient have a cooling effect on near-surface ice temperature. On the other hand, snow and radiative energy input have a warming effect. For this case study, the first three processes

together result in almost no net change so that the modeled T_0 is close to the observed mean air temperature (Fig. 5d). However, inclusion of the subsurface temperature gradient has a strong cooling effect on the simulated temperatures, bringing T_0 far from the mean measured air temperature. The limiting cases show that this bottom boundary condition strongly controls the near-surface temperature, with a range in the resulting T_0 values from -17.0°C to -2.0°C. In summary, measured ice temperatures are consistently warmer than both the measured air temperature and simulated ice temperature (Fig. 6), except in the case of a positive subsurface gradient which is discussed below.

Deleted: ure

Deleted: ure

5 Discussion

Our observations show that measurements of near-surface ice in the ablation zone of western Greenland are significantly warmer than would be predicted by diffusive heat exchange with the atmosphere. This is in agreement with past observations collected in other ablation zones (Hooke et al., 1983). With four experiments in a numerical model that progressively incorporate more physical complexity, we are unable to precisely match independent model output to observations. Our measurement and model output point toward a disconnect between air and ice temperatures in the GrIS ablation zone, with ice temperatures being consistently warmer than the air.

Deleted: e.g.

5.1 Ablation-Diffusion

The strongest result from our model case study was a drop in T_0 by -2.5°C associated with the imposed subsurface temperature gradient. While it was important to test this scenario for one case, the temperature gradient we used was representative but somewhat arbitrary. In reality, the observed temperature gradients are widely variable from one site to another and even within one site (Fig. 2). Interestingly, full ice thickness temperature profiles show similar temperature gradients, both positive and negative (Harrington et al., 2015; Hills et al., 2017). Hence, the limiting cases were added to show simulation results over the range of measured gradients from our temperature strings. The resulting T_0 span a range of 19°C.

Deleted: ure

The majority of the subsurface temperature gradients that we measure are negative, and theoretically the gradient should be negative. Consider that fast horizontal velocities (~100 m/yr) advect cold ice from the divide to the ablation zone, and the air temperature lapse rate couples with the relatively steep surface gradients so that the surface warms rapidly toward the terminus. These conditions lead to a vertical temperature gradient below the ice surface that is negative (Hooke, 2005; pp. 131-135), as in our model example. The one exception is in the case of deep latent heating in a crevasse field (Harrington et al., 2015; sites S3 and S4) where the deep ice temperature is warmer than the mean air temperature rather than colder.

Overall, our results demonstrate that the effect of the subsurface temperature gradient is coupled to that of surface lowering. With respect to the surface, the temperature gradient below is advected upward as ice melts. There is a competition between surface lowering and diffusion of atmospheric energy into the ice; as near-surface ice gets warmer, it can be removed quickly and a new boundary set. Therefore, our conceptualization of temperature in the near-surface ice of the ablation zone should not be a seasonally oscillating upper boundary with purely diffusive heat transfer (Carslaw and Jaeger, 1959), but one with advection and diffusion (Logan and Zlotnik, 1995; Paterson,

Deleted: is warmed

1972). This conceptualization is unique to the ablation zone because of the rapid rate of surface lowering, whereas a diffusive model for near-surface heat transfer is much more appropriate in the accumulation zone.

The disconnect between air and ice temperature implies that the near-surface active layer in the ablation zone is shallow (i.e. less than 15 m) and could be skewed toward the subsurface temperature gradient. Therefore, the surface boundary condition has weak influence on diffusion for ice well below the surface. This is in contrast to the accumulation zone where new snow is advected downward, so the surface temperature quickly influences that at depth. Under these conditions, it is no surprise that we see spatial variability in near-surface ice temperature even within one field site. That variability is simply an expression of the deeper ice temperature variations which are hypothesized to exist from variations in vertical advection (Hills et al., 2017), and do not have time to completely diffuse away before they are exposed at the surface.

5.2 Subsurface Refreezing

We observe heating events in two temperature strings, the largest case being 8°C in 2 hours between 3 and 8 m below the ice surface (Fig. 3c). These events are transient, they are spatially discrete, and they are generated at depth, all of which are most easily explained by the refreezing of liquid water in cold ice. Similar refreezing events have been observed in firn (Humphrey et al., 2012), where they are not only important for ice temperature but could also imply a large storage reservoir for surface meltwater (Harper et al., 2012). However, unlike firn, solid ice is impermeable to water unless fractures are present (Fountain et al., 2005). Two persistently warm features are also observed between 5 and 10 m depth into the winters of 2015 and 2017 (Fig. 3a). We interpret these as a nearby latent heat source, either with running or ponded water that does not freeze for an extended time.

In Greenland's ablation zone, prior work has demonstrated the importance of large-scale latent heating in open crevasses (Phillips et al., 2013; Poinar et al., 2016). Additionally, water-filled cavities have been observed in cold, near-surface ice on mountain glaciers (Jarvis and Clarke, 1974; Paterson and Savage, 1970). In our case, however, an explanation for refreezing water is not obvious. While the field site has occasional mm-aperture 'hairline' cracks, there are no visible open crevasses at the surface for routing water to depth. As far as we know, this work is the first to report evidence of short-term transient latent heating events in cold ice, not obviously linked to open surface fractures.

While the hairline fractures could perhaps move some water, to permit much water to move meters through cold ice they would need to be large enough that water moves quickly and does not instantaneously refreeze. For example, a 1-mm wide crack in ice that is -10°C freezes shut in about 45 seconds (Alley et al., 2005; eq. 8). That amount of time could be long enough for small volumes of water to move 5-10 m below the surface but would require a hydropotential gradient to drive water flow. Thus, top-down hairline crevassing does not seem a plausible explanation for the events we observe.

Importantly, several independent field observations in this area including hole drainage of water during hot-water drilling, ground-penetrating radar reflections, and borehole video observations, all point to the existence of subsurface air-filled and open fractures with apertures of up to a few cm (see Supplement). That they are open at depth, but are narrow or non-existent at the surface, could be linked to the colder ice at depth and its stiffer rheology.

Deleted: In two temperature strings w

Deleted: ure

Deleted: :

Deleted: w

Deleted: s

Nath and Vaughan (2003) observed similar subsurface fractures in firn, although in their case density controls the stiffness rather than temperature. On rare occasions, we argue that the aperture of the fractures open wider to the surface, where there is copious water stored in the cryoconite layer (Cooper et al., 2018) that can drain and refreeze at depth. While the events seem to happen in the springtime and it would be tempting to assert that fracture opening coincides with speedup, our measurements of surface velocity at these sites show that this is not always the case. This may be due to that fact that the spring speedup coincides with early melt rather than peak melt and copious water in the cryoconite layer.

Deleted: crevasses

Latent heating in the form of these subsurface refreezing events is an obvious candidate for a source for the 'extra' heat we observe in our temperature strings relative to simulations. Our data show that refreezing in subsurface fractures has the potential to warm ice substantially over short periods of time, and apparently this can occur in places where open crevasses are not readily observed at the surface. Furthermore, the difference between measured and modeled temperatures (up to 3°C) is the equivalent of only ~1.7% water by volume. Our simplified one-dimensional model would not be well-suited to assess the influence of these latent heating events. Instead, we provide a simple calculation for energy input from the events by differencing the temperature profiles in time and integrating for total energy density (Fig. 7 a-c).

Deleted:

Deleted: crevasses

Deleted: ~

Deleted: ure

$$\phi_{measured} = \frac{\rho_i C_p}{\Delta z} \int \Delta T dz \quad (9)$$

where Δz is the total depth of the profile, and ΔT is the differenced temperature profile. Only sensors that are below the ice surface for the entire time period are considered. To calculate the total water content refrozen in the associated event, we remove the conductive energy fluxes from the total energy density calculated above. We do so by calculating the temperature gradients at the top and bottom of the measured temperature profile at each time step as in Cox et al. (2015).

$$\phi_{conductive} = \frac{-k_i}{\Delta z} \int \left(\frac{\partial T}{\partial z_{top}} - \frac{\partial T}{\partial z_{bottom}} \right) dt \quad (10)$$

The resulting energy sources are then converted to a volume fraction of water by

$$\omega_{measured} = \frac{\phi_{measured} - \phi_{conductive}}{\rho_w L_f} \quad (11)$$

where ρ_w is the density of water. Results show that each year some fractions of a percent of water are refrozen (Fig. 7). Through several seasons that amount of refreezing could easily add up to the ~3°C anomaly that we observe. Unfortunately, without a more thorough investigation, we do not have enough evidence to show that these refreezing events are more than a local anomaly. Of our seven near-surface temperature strings, only T-14 and T-16 demonstrated refreezing events, so we are not confident that they are temporally or spatially ubiquitous. The only other logical mechanism for the warm offset between measurements and model results would be warming from below through a positive subsurface temperature gradient. While it is tempting to associate deep warm ice with residual heat from the exceptionally hot summers of 2010 and 2012 (Tedesco et al., 2013), this scenario is unlikely because the ablation rates are so high that any ice warmed during those years has likely already melted. Deeper

Deleted: ure

Deleted: d-f

Deleted: and

Deleted: ¶

Deleted: ¶

latent heating from an upstream crevasse field is a more plausible alternative; however, in this area full-depth temperature profiles do not show deeper ice to be anomalously warmed except in one localized case (Hills et al., 2017).

6 Conclusion

We observe the temperature of ice at the depth of zero annual amplitude, T_0 , in Greenland's ablation zone to be markedly warmer than the mean annual air temperature. These findings contradict predictions from purely diffusive heat transport but are not surprising considering the processes which impact heat transfer in ice of the ablation zone. High ablation rates in this area indicate that ice temperatures below 15 m reflect the temperature of deep ice that is emerging to the surface, confirming that the ice does not have time to equilibrate with the atmosphere. In other words, ice flow brings cold ice to the surface at a faster rate than heat from the atmosphere can diffuse into the ablating surface. The coupling between rapid ablation and the spatial variability in deep ice temperature implies there will always be a disconnect between air and ice temperatures. Additionally, we observe refreezing events below 5-10 m of cold ice. Meltwater is likely moving to that depth through subsurface fractures that are not obviously visible at the surface.

In analyzing a series of processes that control near-surface ice temperature, we find that some lead to colder ice, and others to warmer, but most are strong enough to dramatically alter the ice temperature from the purely diffusive case. With rapid ablation, a spatially variable temperature field, and subsurface refreezing events, T_0 in the ablation zone should not be expected to match the air temperature. That our measurements are consistently warmer, could simply be due to the limited number of observations we have, but latent heat additions are clearly measured and could be common in near-surface ice of the western Greenland ablation zone.

References

- Alley, R. B., Dupont, T. K., Parizek, B. R., and Anandakrishnan, S. (2005). Access of surface meltwater to beds of sub-freezing glaciers: Preliminary insights. *Annals of Glaciology*, 40, 8–14. doi:10.3189/172756405781813483
- van As, D., Hubbard, A. L., Hasholt, B., Mikkelsen, A. B., van den Broeke, M. R., and Fausto, R. S. (2012). Large surface meltwater discharge from the Kangerlussuaq sector of the Greenland ice sheet during the record-warm year 2010 explained by detailed energy balance observations. *The Cryosphere*, 6(1), 199–209. doi:10.5194/tc-6-199-2012
- Aschwanden, A., Bueller, E., Khroulev, C., and Blatter, H. (2012). An enthalpy formulation for glaciers and ice sheets. *Journal of Glaciology*, 58(209), 441–457. doi:10.3189/2012JoG11J088
- Brandt, R., and Warren, S. (1993). Solar-heating rates and temperature profiles in Antarctica snow and ice. *Journal*

Deleted: ~

of *Glaciology*, 39(131), 99–110.

- Brinkerhoff, D. J., and Johnson, J. V. (2013). Data assimilation and prognostic whole ice sheet modelling with the variationally derived, higher order, open source, and fully parallel ice sheet model VarGlaS. *The Cryosphere*, 7(4), 1161–1184. doi:10.5194/tc-7-1161-2013
- van den Broeke, M., Smeets, P., Ettema, J., Van Der Veen, C., Van De Wal, R., and Oerlemans, J. (2008). Partitioning of melt energy and meltwater fluxes in the ablation zone of the west Greenland ice sheet. *The Cryosphere*, 2, 179–189. doi:10.5194/tc-2-179-2008
- Calonne, N., Flin, F., Morin, S., Lesaffre, B., Du Roscoat, S. R., and Geindreau, C. (2011). Numerical and experimental investigations of the effective thermal conductivity of snow. *Geophysical Research Letters*, 38(23), 1–6. doi:10.1029/2011GL049234
- Carslaw, H. S., and Jaeger, J. C. (1959). *Conduction of Heat in Solids (Second)*. London: Oxford University Press.
- Cooper, M. G., Smith, L. C., Rennermalm, A. K., Mige, C., Pitcher, L. H., Ryan, J. C., ... Cooley, S. W. (2018). Meltwater storage in low-density near-surface bare ice in the Greenland ice sheet ablation zone. *The Cryosphere*, 12(3), 955–970. doi:10.5194/tc-12-955-2018
- Cox, C., Humphrey, N., and Harper, J. (2015). Quantifying meltwater refreezing along a transect of sites on the Greenland ice sheet. *The Cryosphere*, 9, 691–701. doi:10.5194/tc-9-691-2015
- Cuffey, K., and Paterson, W. S. B. (2010). *The Physics of Glaciers (Fourth)*. Oxford, UK: Butterworth-Heinemann.
- van Everdingen, R. O. (1998). *Multi-language glossary of permafrost and related ground-ice terms*. Calgary, Alberta, CA: International Permafrost Association.
- Fountain, A. G., Jacobel, R. W., Schlichting, R., and Jansson, P. (2005). Fractures as the main pathways of water flow in temperate glaciers. *Nature*, 433(7026), 618–621. doi:10.1038/nature03296
- Harper, J. T., Humphrey, N. F., Pfeffer, W. T., Brown, J., and Fettweis, X. (2012). Greenland ice-sheet contribution to sea-level rise buffered by meltwater storage in firn. *Nature*, 491, 240–243. doi:10.1038/nature11566
- Harrington, J. a, Humphrey, N. F., and Harper, J. T. (2015). Temperature distribution and thermal anomalies along a flowline of the Greenland Ice Sheet. *Annals of Glaciology*, 56(70), 98–104. doi:10.3189/2015AoG70A945
- Hills, B. H., Harper, J. T., Humphrey, N. F., and Meierbachtol, T. W. (2017). Measured horizontal temperature gradients constrain heat transfer mechanisms in Greenland ice. *Geophysical Research Letters*, 44(19). doi:10.1002/2017GL074917

- Hooke, R. L. (1976). Near-surface temperatures in the superimposed ice zone and lower part of the soaked zone of polar ice sheets. *Journal of Glaciology*, 16(74), 302–304.
- Hooke, R. L. (2005). *Principles of Glacier Mechanics (Second)*. Cambridge University Press.
- Hooke, R. L., Gould, J. E., and Brzozowski, J. (1983). Near-surface temperatures near and below the equilibrium line on polar and subpolar glaciers. *Zeitschrift Für Gletscherkunde Und Glazialgeologie*, 1–25.
- Howat, I. M., Negrete, A., and Smith, B. E. (2014). The Greenland Ice Mapping Project (GIMP) land classification and surface elevation data sets. *The Cryosphere*, 8(4), 1509–1518. doi:10.5194/tc-8-1509-2014
- Humphrey, N. F., Harper, J. T., and Pfeffer, W. T. (2012). Thermal tracking of meltwater retention in Greenland's accumulation area. *Journal of Geophysical Research*, 117, 1–11. doi:10.1029/2011JF002083
- Jarvis, G. T., and Clarke, G. K. C. (1974). Thermal effects of crevassing on Steele Glacier, Yukon Territory, Canada. *Journal of Glaciology*, 13(68), 243–254.
- Liston, G. E., Winther, J.-G., Bruland, O., Elvehoy, H., and Sand, K. (1999). Below-surface ice melt on the coastal Antarctic ice sheet. *Journal of Glaciology*, 45(150), 273–285.
- Lliboutry, L. (1965). *Traité de Glaciologie*. Paris: Masson. doi:10.1002/qj.49709439916
- Loewe, F. (1970). Screen temperatures and 10 m temperatures. *Journal of Glaciology*, 9(56), 263–268.
- Logan, J. D., and Zlotnik, V. (1995). The convection-diffusion equation with periodic boundary conditions. *Applied Mathematics Letters*, 8(3), 55–61. doi:10.1016/0893-9659(95)00030-T
- Lüthi, M. P., Ryser, C., Andrews, L. C., Catania, G. a., Funk, M., Hawley, R. L., ... Neumann, T. a. (2015). Heat sources within the Greenland Ice Sheet: dissipation, temperate paleo-firn and cryo-hydrologic warming. *The Cryosphere*, 9(1), 245–253. doi:10.5194/tc-9-245-2015
- Lüthi, M., Funk, M., Iken, A., Gogineni, S., and Truffer, M. (2002). Mechanisms of fast flow in Jakobshavns Isbrae, West Greenland: Part III. measurements of ice deformation, temperature and cross-borehole conductivity in boreholes to the bedrock. *Journal of Glaciology*, 48(162), 369–385.
- Meierbachtol, T. W., Harper, J. T., Johnson, J. V., Humphrey, N. F., and Brinkerhoff, D. J. (2015). Thermal boundary conditions on western Greenland: Observational constraints and impacts on the modeled thermomechanical state. *Journal of Geophysical Research: Earth Surface*, 120, 623–636. doi:10.1002/2014JF003375. Received

- Miller, N. B., Turner, D. D., Bennartz, R., Shupe, M. D., Kulie, M. S., Cadeddu, M. P., and Walden, V. P. (2013). Surface-based inversions above central Greenland. *Journal of Geophysical Research: Atmospheres*, 118(2), 495–506. doi:10.1029/2012JD018867
- Mock, S. J., and Weeks, W. F. (1966). The distributio of 10 meter snow temperatures on the Greenland Ice Sheet. *Journal of Glaciology*, 6(43), 23–41.
- Müller, F. (1976). On the thermal regime of a high-arctic valley glacier. *Journal of Glaciology*, 16(74), 119–133.
- Nath, P. C., and Vaughan, D. G. (2003). Subsurface crevasse formation in glaciers and ice sheets. *Journal of Geophysical Research*, 108(B1), 1–12. doi:10.1029/2001JB000453
- Paterson, W. S. B. (1972). Temperature distribution in the upper layers of the ablation area of Athabasca Glacier, Alberta, Canada. *Journal of Glaciology*, 11(61), 31–41.
- Paterson, W. S. B., and Savage, J. C. (1970). Excess pressure observed in a water-filled cavity in Athabasca Glacier, Canada. *Journal of Glaciology*, 9(95), 103–107.
- Perovich, D. K. (2007). Light reflection and transmission by a temperate snow cover. *Journal of Glaciology*, 53(181), 201–210. doi:10.3189/172756507782202919
- Phillips, T., Rajaram, H., Colgan, W., Steffen, K., and Abdalati, W. (2013). Evaluation of cryo-hydrologic warming as an explanation for increased ice velocities in the wet snow zone, Sermeq Avannarleq, West Greenland. *Journal of Geophysical Research: Earth Surface*, 118(3), 1241–1256. doi:10.1002/jgrf.20079
- Phillips, T., Rajaram, H., and Steffen, K. (2010). Cryo-hydrologic warming: A potential mechanism for rapid thermal response of ice sheets. *Geophysical Research Letters*, 37(20), 1–5. doi:10.1029/2010GL044397
- Poinar, K., Joughin, I., Lenaerts, J. T. M., and van den Broeke, M. R. (2016). Englacial latent-heat transfer has limited influence on seaward ice flux in western Greenland. *Journal of Glaciology*, 1–16. doi:10.1017/jog.2016.103
- Tedesco, M., Fettweis, X., Mote, T., Wahr, J., Alexander, P., Box, J., and Wouters, B. (2013). Evidence and analysis of 2012 Greenland records from spaceborne observations, a regional climate model and reanalysis data. *The Cryosphere*, 7, 615–630. doi:10.5194/tcd-6-4939-2012
- van de Wal, R. S. W., Boot, W., Smeets, C. J. P. P., Snellen, H., van den Broeke, M. R., and Oerlemans, J. (2012). Twenty-one years of mass balance observations along the K-transect, West Greenland. *Earth System Science Data*, 4(1), 31–35. doi:10.5194/essd-4-31-2012

Warren, S. G. (1982). Optical properties of snow. *Reviews of Geophysics*. doi:10.1029/RG020i001p00067

Wientjes, I. G. M., and Oerlemans, J. (2010). An explanation for the dark region in the western melt zone of the Greenland ice sheet. *The Cryosphere*, 4(3), 261–268. doi:10.5194/tc-4-261-2010

Yen, Y.-C. (1981). Review of thermal properties of snow, ice, and sea ice. CRREL Report 81-10. Retrieved from <http://acwc.sdp.sirsi.net/client/search/asset/1005644>

Figure 1: A site map from southwest Greenland with field sites (red) named by their location with respect to the outlet terminus of Isunnguata Sermia. The inset shows locations of near-surface temperature strings (black) named by the year they were installed and an automated weather station (blue). Surface elevation contours are shown at 200-m spacing (Howat et al., 2014).

Figure 2: Near-surface ice temperature measurements from seven strings: T-11a, T-11b, T-14, T-15a, T-15b, T-15c, and T-16. For each, the shaded region shows the range of measured temperatures over the entire measurement period, and the solid line indicates the mean temperature profile. Depths are plotted with respect to the surface at the time of measurement, so sensor locations move toward the surface as ice melts. Strings with less than 11 months of data are slightly more transparent. For field sites at which the air temperature was measured for at least a full year, a dashed line shows the mean air temperature.

Figure 3: Three years of ice temperature measurements from the T-14 string. While this string was initially installed to 21-m depth, measurements are plotted with reference to the moving surface, so the sensors move up throughout the time period, revealing a gray mask. Transient features in the data include anomalously slow freeze-in behavior in one sensor (b) as well as heating events throughout the collection time period (c, d, and e). The heating events are plotted as a series of temperature profiles with the darker shades being later times and time steps between profiles of 2 hours (c), 10 hours (d), and 1 hour (e).

Figure 4: Heating events from temperature string T-16. Profiles are plotted as in Figure 3 c, d, and e. The time steps between profiles are 2 hours (a) and 4 hours (b).

Figure 5: Model results for five separate simulations. In each case, twelve simulated temperature profiles are shown from throughout the year-long period, and control results (from (a)) are displayed for comparison (gray). Differences between the simulations are analyzed quantitatively using T_b , the convergent temperature at 21 m. Processes are, from top to bottom: a) control simulation of pure diffusion, b) ablation, c) snow insulation, d) radiative energy input, and finally e) subsurface temperature gradient. The two limiting cases for the subsurface temperature gradient are plotted with dashed gray lines (e).

Figure 6: A comparison of model output (gray) and data from 33-km, including mean ice temperatures (red) and

mean annual air temperatures for three seasons (black dashed). The observed ice temperatures are plotted the same as in Figure 2. Note that three of the temperature strings collected only ~9 months of data (transparent red). Mean temperatures from those three strings are cold near the surface because they collected more wintertime measurements than summertime.

Figure 7: Energy source for the observed heating events. a-c) Observed energy density through time for the differenced temperature profile calculated with equation (9) (black), and conductive energy density through time calculated with equation (10) (red). d-f) Percent by volume water refrozen for the associated source in (a-c). This value is proportional to the difference between the black and red lines above. The temperature string from which measurements were taken is labeled at the top.

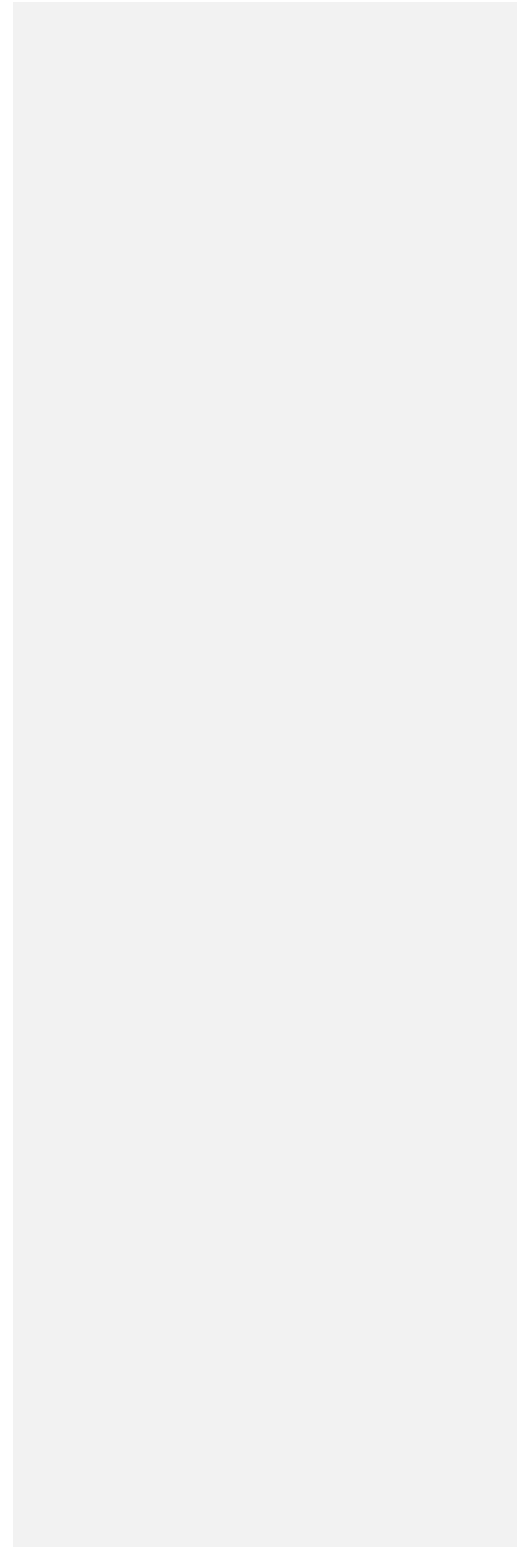


Table 1: Temperature Strings

String Name	Data Time Period	Time Step (hr)	Sensor	# of Sensors	Sensor Spacing (m)	Latitude	Longitude	Elevation (m)
T-11a	7/5/11 – 7/15/13	3	Thermistor	32	0.6	67.195175	-49.719515	848
T-11b	7/11/11 – 12/17/11	3	Thermistor	32	0.6	67.201553	-49.289058	1095
T-14	7/18/14 – 6/23/17	0.5	Thermistor	31	< 11 m deep – 0.5 > 11 m deep – 1.0	67.18127	-49.56982	956
T-15a	8/17/16 - 5/20/17	0.5	DS18B20	17	< 15 m deep – 1.0 > 15 m deep – 3.0	67.18211	-49.568272	954
T-15b	8/17/16 - 5/20/17	0.5	DS18B20	17	< 15 m deep – 1.0 > 15 m deep – 3.0	67.182054	-49.568059	954
T-15c	8/17/16 - 5/20/17	0.5	DS18B20	17	< 15 m deep – 1.0 > 15 m deep – 3.0	67.182114	-49.568484	954
T-16	8/17/16 - 7/22/17	0.5	DS18B20	18	0.5	67.18147	-49.57025	951

|

Table 2: Constants

Variable	Symbol	Value	Units	Reference
Reference Enthalpy	H_m	0	J kg^{-1}	
Ice Density	ρ_i	917	kg m^{-3}	Cuffey and Paterson (2010)
Snow Density	ρ_s	300	kg m^{-3}	
Water Density	ρ_w	1000	kg m^{-3}	
Specific Heat Capacity	C_p	2097	$\text{J kg}^{-1} \text{K}^{-1}$	Cuffey and Paterson (2010)
Latent Heat of Fusion	L_f	$3.335 \cdot 10^5$	J kg^{-1}	Cuffey and Paterson (2010)
Thermal Conductivity of Ice	k_i	2.1	$\text{J m}^{-1} \text{K}^{-1} \text{s}^{-1}$	Cuffey and Paterson (2010)
Thermal Conductivity of Snow	k_s	0.2	$\text{J m}^{-1} \text{K}^{-1} \text{s}^{-1}$	Calonne et al. (2011)
Moisture Diffusivity	ν	$1 \cdot 10^{-4}$	$\text{kg m}^{-1} \text{s}^{-1}$	Aschwanden et al. (2012)